

Mahendra Singh¹, Anuj Kumar², Naresh Kumar³, Poonam Tandon³ and Vishwambhar Dayal Gupta⁴

A STUDY OF VIBRATIONAL DYNAMICS OF POLY (α -N-BUTYL- β -L-ASPARTATE) (PANBLA)

¹ Department of Physics, Brahmanand P.G. College, 224 008 Kanpur, India.

² Jaypee Institute of Eng. and Technology, Guna, MP, 473226 India

³ Department of Physics, University of Lucknow, 226 007 Lucknow, India.

⁴ Department of Physics, Integral University, 226026 Lucknow, India

Received: May 05, 2008

© Singh M., Kumar A., Kumar N., Tandom P., Gupta V.D. 2009

Abstract. Poly(α -n-butyl- β -L-aspartate) (PANBLA) is nylon-3 derivative in which an alcoxycarbonyl group has been stereoregularly attached to β -carbon of the repeating unit. Like poly(α -isobutyl- β -L-aspartate) (PAIBLA) exists in two helical forms, namely hexagonal form (13/4 helix) and tetragonal form (4/1 helix), were characterized by X-ray diffraction. The hexagonal form appears to be poorly crystalline and it could not be obtained well oriented. On the other hand tetragonal form turns to be highly crystalline. Both molecular mechanics calculations and the linked-atom least square (LALS) methodology using X-ray diffraction data have revealed that an antiparallel packing of 13/4 helices with a right handed (2R) scheme of hydrogen bonds is most favourable for hexagonal form of PANBLA. Regarding tetragonal form the above techniques favour a parallel arrangement of 4/1 helices according to right handed 4R model. IR dichroism studies also support the above results. Although the vibrational dynamics of both forms of PAIBLA has been studied, no such study has been performed for PANBLA. In the present communication the vibrational dynamics of PANBLA in tetragonal form (4/1 helix) has been studied through the dispersion of normal modes. The effect of side chain nature on the dynamical behaviour has also been analyzed. Apart from detailed assignments of modes, various characteristic features of dispersion curves have been explained as arising due to internal symmetry in energy momentum space. Finally, the density of states has been used to calculate heat capacity of this polymer.

Key words: poly(α -n-butyl β -L-aspartate), density of states, phonon dispersion, heat capacity

1. Introduction

Polyamides have an amide group and varying number of carbon atoms in their chemical repeat unit.

These polymers like polypeptides have a tendency to go into helical conformation and get stabilized by hydrogen bonding scheme [1]. Polyamides with three carbon atoms present in their repeat unit are called nylon-3 derivatives. Poly (β -L-aspartates) family, which is a derivative of nylon-3, has been systematically investigated by Fernandez-Santin *et al.* [2].

Poly(α -alkyl- β -L-aspartate)s are nylon-3 derivatives in which an alcoxycarbonyl group has been stereoregularly attached to the β -carbon of the repeating unit. A number of new polyamides with structure and properties intermediate between nylons and polypeptides can be generated by different modifications. These poly(β -amides) can adopt α -helix type conformation, which is generally characteristic of polypeptides and proteins [3-5]. The additional methylene unit in the backbone chain offers greater freedom to the conformational angle and allows different helical conformations. Most of the nylon-3 derivatives like poly (α -isobutyl- β -L-aspartate) (PAIBLA) [2] and poly(α -n-butyl- β -L-aspartate) (PANBLA) [6] show two types of helical structures (13/4 and 4/1 helices)

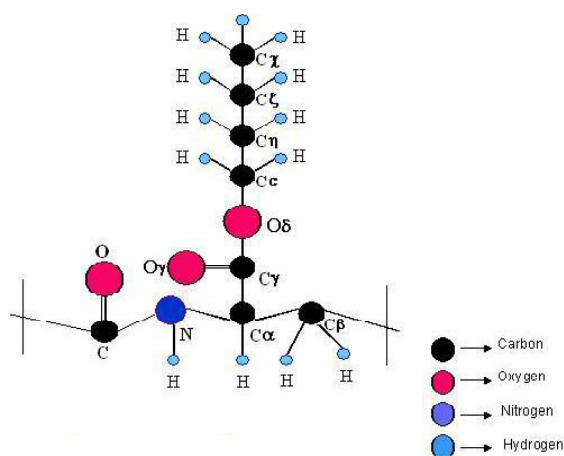


Fig. 1. One chemical repeat unit of PANBLA

whereas conventional polypeptides are generally present only in the α -helical structure. Polyamides related to nylon-3 have attracted interest as they yield fibres with properties close to the natural silk [7].

PANBLA (Fig. 1) is an n-butyl derivative of poly(β -aspartic acid) ester. Like PAIBLA two helical forms, namely hexagonal form (13/4 helix) and tetragonal form (4/1 helix) bearing a structural resemblance to the polypeptide α -helix, were characterized by X-ray diffraction [6]. Preparation conditions determine the structural forms [8]. The hexagonal form appears to be poorly crystalline and it could not be obtained well oriented. On the other hand tetragonal form turns out to be highly crystalline [6]. Both molecular mechanics calculations and the linked-atom least square (LALS) methodology using X-ray diffraction data [9] have revealed that an anti-parallel packing of 13/4 helices with a right handed (2R) scheme of hydrogen bonds is most favourable for hexagonal form of PANBLA. Regarding the tetragonal form, the above techniques favour a parallel arrangement of 4/1 helices according to right handed 4R model [6]. IR dichroism studies also support the above results [10]. The relative stabilities of two forms are mainly determined by Vander Waals and electrostatic interactions. The contribution of Vander Waals term is clearly in favour of the tetragonal form in PANBLA whereas the reverse is observed to occur in PAIBLA [9].

Though the two forms of PANBLA are basically identical to those reported for PAIBLA, the crystal transition from hexagonal to tetragonal by heating is not observed in case of PANBLA. However, like in PAIBLA, conversion can be induced by alcohols in PANBLA as well. Both hexagonal and tetragonal forms show helix coil transition similar to that found in helical polypeptides and PAIBLA [2].

2. Experimental

Vibrational spectroscopy is one of the most used methods to study the polymers. It can be used to determine crystallinity, conformation, intra and intermolecular hydrogen bonding, fold structure of polymers, composition and sequence distribution in copolymers. Normal mode analysis has been performed for both tetragonal and hexagonal forms of PAIBLA to understand the dynamical behaviour [11-12]. However, no such work has been done for PANBLA. In the present work we report a detailed vibrational dynamics of PANBLA in tetragonal form. We have used the FT-IR spectra (Fig.2) recorded by us for assignment of different modes. Various features of dispersion curves such as repulsions, exchange of character, *etc.* are discussed in terms of symmetry considerations. Further the frequency distribution function obtained from dispersion curves may be used to correlate the microscopic behaviour with macroscopic properties. Heat capacity has been calculated in the range 50–500 K via density-of-states.

2.1. Calculation of Normal Mode Frequencies

Normal mode calculation for an isolated polymeric chain was carried out using Wilson's GF matrix [13] method as modified by Higgs [14] for an infinite polymeric chain. The vibrational secular equation to be solved is:

$$|G(d)F(d) - I(d)I| = 0 \quad 0 \leq d \leq p \quad (1)$$

where d is the phase difference between the modes of adjacent chemical units, $G(d)$ is the inverse kinetic energy matrix and

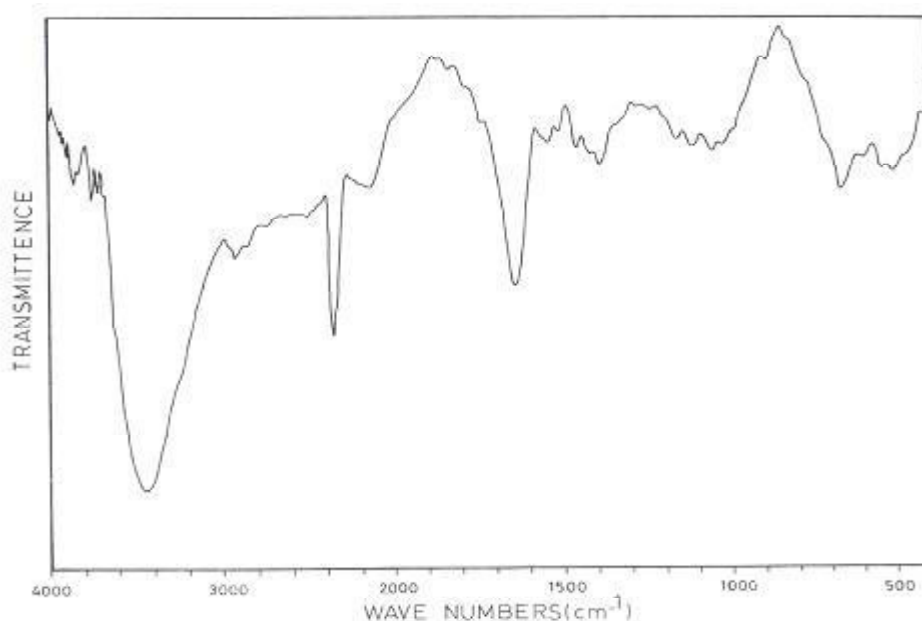


Fig. 2. FT-IR spectra of PANBLA (4000–450 cm^{-1})

$F(d)$ is the force field matrix for a certain phase value. The frequencies n_i in cm^{-1} are related to eigen values by

$$I_i(d) = 4p^2 c^2 n_i^2(d) \quad (2)$$

A plot of $n_i(d)$ versus d gives the dispersion curve for the i^{th} mode. The use of the type of force field is generally a matter of one's chemical experience and intuition [15]. In the present work we used the Urey-Bradley force field (UBFF), as it is more comprehensive than the valence force field. In the UBFF (1) relatively fewer parameters are required to express the potential energy, (2) no quadratic terms cross terms are included, the interaction between non-bonded atoms in gem and tetra-configuration can be included and (3) the arbitrariness in choosing the force constant is reduced.

2.2. Calculation of Heat Capacity

Dispersion curves can be used to calculate the specific heat of a polymeric system. For a one-dimensional system, the density-of-states function or the frequency distribution function expresses the way energy is distributed among various branches of normal modes in the crystal and is calculated from the relation:

$$g(n) = \sum_j \left(\frac{\partial n_j}{\partial d} \right)_{n_j(d)=n_j}^{-1} \quad (3)$$

The sum is taken over all the dispersion branches j . Considering a solid as an assembly of harmonic oscillators, the frequency distribution $g(n)$ is equivalent to a partition function. The constant volume heat capacity can be calculated using Debey's relation:

$$C_v = \sum g(n_j) K N_A (h n_j / KT)^2 \cdot \frac{\exp(h n_j / KT)}{(\exp(h n_j / KT) - 1)^2}$$

with $\int g(n_i) dn_i = 1$ (4)

The Fourier transform infrared (FT-IR) spectra (Fig. 2) of PANBLA has been recorded on Perkin-Elmer 1800 spectrometer in the range 4000–450 cm^{-1} . The sample was prepared by mixing it in CsI and pressing in the form of a pellet. Before recording the spectra, the equipment was purged with dry nitrogen.

3. Results and Discussion

One residue unit of PANBLA (Fig.1) contains 25 atoms, which give rise to 75 dispersion curves. Initially the force constants were transferred from PAIBLA [11] (tetragonal form) and systems having similar environment and then refined to give the "best" fit to the FT-IR spectra (see Fig. 2). The assignments were made on the basis of

potential energy distribution (PED), band profile, band intensities, and the presence/absence of similar groups in an identical environment. The final force constants are given in Table 1. The vibrational frequencies have been calculated for the values of d ranging from 0 to p in steps of 0.05π . The optically active modes correspond to those at $d=0$, $d=\varphi$ (helix angle) and 2φ , where φ is the angle of rotation around the helix axis which separates the adjacent units. The modes corresponding to $d=0$ and φ are both Raman and IR active while modes belonging to $d=2\varphi$ are only Raman active. In tetragonal form (4/1helix), there are four residue units per turn with helix angle equal to $0.50p$. Although the spectrum is not available below 450 cm^{-1} , calculations are expected to be correct for more than one reason. First, they occur in the same range, as these modes in other systems do [11-12]. Second, since the force constants which are involved in low frequency region are also involved in the higher frequency region wherein they yield "good" frequencies, the results in this frequency region should also have a reasonably close predictive value. A check can be provided by spectral observations in the far IR region.

The modes above 900 cm^{-1} are either non-dispersive or show very little dispersion so they are not shown. The dispersion curves below this region are shown in Figs. 3a, 4a and 5a, and corresponding density-of-states are plotted in Figs. 3b, 4b and 5b. The dispersion curves shown in Fig 5a have four zero frequencies, two at $d=0$, corresponding to translational mode along chain axis and rotational mode along helix axis, the other two degenerate zero modes at $d=0.50p$ (helix angle) belong to translations perpendicular to the helix axis. For convenience, the modes are discussed under three separate heads, viz. backbone modes, side chain modes and mixed modes, which are shown in Tables 2, 3 and 4 respectively.

3.1. Backbone Modes

The vibrational modes involving the motion of main chain atoms ($-\text{CO}-\text{NH}-\text{C}_\alpha-\text{C}_\beta-$) are termed as backbone modes. The PEDs of these modes along with their assignments at $d=0$ and $0.5p$ are given in Table 2. These modes are mostly amide modes.

3.2. Amide Modes

The amide groups of polypeptides are strongly chromatophoric in IR-absorption and give rise to strong characteristic bands (amide A, I–VII). These modes along with the other characteristic modes have been used for the determining conformation of proteins and polypeptides.

The amide A band, due to N–H stretching vibration is calculated at 3287 cm^{-1} and assigned to the observed peak [10] at the same value. It is highly sensitive to the strength of N–H...O=C hydrogen bond. This bond plays

crucial role in determining structure and properties of a great variety of compounds like peptides, proteins and synthetic polyamides. The amide I mode, which is predominately due to C=O and C=N stretches, is calculated at 1643 cm⁻¹ (at $d = 0$) and assigned to the observed absorption peak at 1644 cm⁻¹. The amide II mode (N-H in plane bend and C=N stretch) has been calculated at 1548 cm⁻¹, which corresponds to the observed peak at 1550 cm⁻¹. These all modes (amide A, I, II) are nondispersive in the energy momentum space. The amide III mode calculated at 1272 cm⁻¹ at the zone center is assigned to the observed peak at 1278 cm⁻¹. This mode disperses with progressive d value and at the helix angle it reaches 1265 cm⁻¹ showing dispersion by 7 cm⁻¹. This mode is affected by the nature of side chain. As d increases, the contribution of $\varphi(\text{H-C}\alpha\text{-C}\gamma)$ increases, showing coupling of the side chain.

The observed peak at 669 cm⁻¹ matches well with the calculated frequency at 668 cm⁻¹ having contributions of N-H out-of-plane and C=O in plane bending (amide V + IV). The calculated frequency at 549 cm⁻¹ ($d = 0$) is assigned to the observed peak at the same value. This mode has dominant contribution of C=O out of plane bending (amide VI). Amide IV, V, VI are mixed with side chain modes and due to electrical as well as mechanical coupling between backbone and side chains, they have dispersive nature.

We have compared the amide modes of PANBLA with other w helical conformations such as PAIBLA [11], poly(N ^{ϵ} -*p*-bromobenzyl-L-ornithine) (PBrBO) [16], poly(L-phenylalanine) (PLPA) [17] as shown in Table 5. Some differences in lower range may be due to mixing of amide modes in this region. A comparison between various amide modes of PANBLA (4/1 helix) with 4/1 and 13/4 helices of PAIBLA is also given in Table 6.

Table 1

Internal coordinates and force constants for PANBLA (mydne/ Å)

Internal coordinates	Force constants	Internal coordinates	Force constants
ν (C=N)	5.68	φ (C α -C γ -O γ)	0.36 (0.600)
ν (C=O)	6.61	φ (C α -C γ -O δ)	0.33 (0.500)
ν (N-H)	5.272	φ (O γ -C γ -O δ)	0.15 (0.800)
ν (N-C α)	3.85	φ (C γ -O δ -C ϵ)	0.26 (0.450)
ν (C α -H)	4.246	φ (O δ -C ϵ -C η)	0.33 (0.500)
ν (C α -C β)	2.70	φ (O δ -C ϵ -H)	0.46 (0.250)
ν (C α -C γ)	2.45	φ (H-C ϵ -H)	0.426 (0.250)
ν (C β -H)	4.24	φ (H-C ϵ -C η)	0.510 (0.180)
ν (C β -C)	2.45	φ (C ϵ -C η -C ξ)	0.510 (0.180)
ν (C γ -O δ)	3.55	φ (C ϵ -C η -H)	0.520 (0.220)
ν (C γ -O γ)	1.095	φ (H-C η -H)	0.418 (0.241)
ν (O δ -C ϵ)	3.50	φ (H-C η -C ξ)	0.485 (0.180)
ν (C ϵ -H)	4.20	φ (C η -C ξ -C χ)	0.51 (0.180)
ν (C ϵ -C η)	3.10	φ (C η -C ξ -H)	0.485 (0.220)
ν (C η -C ξ)	2.75	φ (H-C ξ -H)	0.420 (0.237)
ν (C η -H)	4.218	φ (H-C ξ -C χ)	0.560 (0.180)
ν (C ξ -C χ)	2.95	φ (C ξ -C χ -H)	0.465 (0.170)
ν (C ξ -H)	4.22	φ (H-C χ -H)	0.423 (0.242)
ν (C χ -H)	4.365	φ (C β -C=O)	0.236 (0.600)
φ (O=C=N)	0.55 (0.900)	φ (C β -C=N)	0.210 (0.600)
φ (C=N-C α)	0.53 (0.350)	ω (C=O)	0.410
φ (C=N-H)	0.442 (0.650)	ω (N-H)	0.10
φ (H-N-C α)	0.222 (0.600)	ω (C γ -O γ)	0.323
φ (N-C α -C β)	0.13 (0.500)	τ (N-C α)	0.020
φ (N-C α -C γ)	0.40 (0.500)	τ (C α -C γ)	0.050
φ (N-C α -H)	0.288 (0.800)	τ (C γ -O δ)	0.060
φ (H-C α -C β)	0.42 (0.200)	τ (O δ -C ϵ)	0.0285
φ (H-C α -C γ)	0.52 (0.200)	τ (C ϵ -C η)	0.028
φ (C γ -C α -C β)	0.52 (0.180)	τ (C η -C ξ)	0.030
φ (C α -C β -C)	0.55 (0.180)	τ (C ξ -C χ)	0.012
φ (C α -C β -H)	0.36 (0.200)	τ (C α -C β)	0.010
φ (H-C β -C)	0.38 (0.200)	τ (C β -C)	0.023
φ (H-C β -H)	0.45 (0.200)	τ (C=N)	0.058

Note: ν , φ , ω and τ denote stretch, angle bend, wag and torsion, respectively. Non-bonded force constants are given in parentheses.

Table 2

Pure backbone modes in PANBLA

Cal. freq.	FTIR Exp. freq.	Assignment ($\delta = 0$) PED (%)	Cal. freq.	Obs. freq.	Assignment ($\delta = 0.50\pi$) PED (%)
3287	3287	ν [N-H](100)	3287	3287	ν [N-H](100)
2965	2967	ν [C α -H](99)	2965	2967	ν [C α -H](99)
2899	--	ν [C β -H](99)	2899	--	ν [C β -H](99)
2859	2868	ν [C β -H](100)	2859	2868	ν [C β -H](100)
1644	1643	ν [C=O](46)+ ν [C-N](39)	1643	1643	ν [C=O](46)+ ν [C-N](39)
1548	1550	ϕ [C-N-H](43)+ ϕ [H-N-C α](29)+ ν [C-N](14)+ ν [N-C α](8)	1548	1550	ϕ [C-N-H](43)+ ϕ [H-N-C α](29)+ ν [C-N](14)+ ν [N-C α](8)
1426	1428	ϕ [H-C β -H](80)+ ϕ [H-C β -C](13)	1426	1428	ϕ [H-C β -H](79)+ ϕ [H-C β -C](13)
1272	1278	ν [N-C α](22)+ ν [C-N](13)+ ν [C=O](12)+ ν [C β -C](10)+ ϕ [N-C α -H](9)+ ϕ [H-N-C α](8)+ ϕ [O=C-N](7)	1265	1278	ν [N-C α](24)+ ν [C-N](9)+ ν [C=O](9)+ ϕ [H-C α -C β](8)+ ϕ [H-C α -C γ](7)
1156	1158	ν [N-C α](28)+ ν [C-N](16)+ ϕ [C α -C β -H](12)+ ν [C=O](9)+ ϕ [H-C β -C](8)+ ν [C α -C β](7)+ ν [C β -C](6)	1156	1158	ν [N-C α](23)+ ϕ [C α -C β -H](16)+ ν [C-N](13)+ ϕ [H-C β -C](11)+ ν [C=O](9)+ ν [C α -C β](5)
1057	1050	ϕ [H-C β -C](52)+ ϕ [C α -C β -H](34)+ ν [N-C α](7)	1050	1050	ϕ [H-C β -C](49)+ ϕ [C α -C β -H](33)+ ν [N-C α](9)
956	960	ν [C α -C β](50)+ ϕ [H-C α -C β](6)+ ν [C β -H](6)	952	960	ν [C α -C β](50)+ ϕ [H-C α -C β](10)+ ϕ [C α -C β -H](5)+ ϕ [C-N-C α](5)
881	876	ν [C β -C](37)+ ν [C=O](13)+ ϕ [O=C-N](8)+ ϕ [H-C β -C](6)+ ν [C α -C β](6)+ ϕ [C α -C β -H](6)+ ν [C-N](6)	881	876	ν [C β -C](38)+ ν [C=O](13)+ ϕ [O=C-N](7)+ ϕ [H-C β -C](6)
668	669	ω [N-H](19)+ ϕ [O=C-N](11)+ ϕ [C=O](9)+ ϕ [H-C β -C](8)+ ϕ [C α -C β -C](8)+ ϕ [C-N-C α](5)	662	669	ω [N-H](13)+ ϕ [O=C-N](12)+ ω [C γ -O γ](7)+ ω [C=O](7)+ ϕ [C α -C β -C](6)+ ϕ [C-N-C α](6)
549	549	ω [C=O](37)+ ϕ [O=C-N](7)+ τ [N-C α](7)	554	549	ω [C=O](24)+ ϕ [O γ =C γ -O δ](12)+ ω [C γ -O γ](7)+ τ [N-C α](6)
0	--	ϕ [H-N-C α](20)+ ϕ [C-N-C α](16)+ ϕ [C-N-H](15)+ τ [N-C α](5)+ τ [C β -C](14)	3	--	τ [C α -C β](29)+ ω [N-H](16)+ τ [N-C α](8)+ τ [C β -C](7)+ ϕ [N-C α -C β](6)

Note: All frequencies are in cm⁻¹.

Table 4

Mixed modes in PANBLA

Cal. freq.	Obs. freq.	Assignment ($d = 0$) PED (%)	Cal. freq.	Obs. freq.	Assignment ($d = 0.50p$) PED (%)
1346	1347	$\phi[\text{N-C}\alpha\text{-H}](51)+\phi[\text{H-C}\alpha\text{-C}\gamma](21)+\nu[\text{N-C}\alpha](9)$	1347	1347	$\phi[\text{N-C}\alpha\text{-H}](51)+\phi[\text{H-C}\alpha\text{-C}\gamma](21)+\nu[\text{N-C}\alpha](9)$
1283	1278	$\phi[\text{H-C}\alpha\text{-C}\beta](15)+\nu[\text{C}\alpha\text{-C}\beta](10)+\phi[\text{H-C}\eta\text{-C}\xi](10)+\phi[\text{C}\varepsilon\text{-C}\eta\text{-H}](9)+\phi[\text{H-C}\alpha\text{-C}\gamma](8)+\phi[\text{C}\alpha\text{-C}\beta\text{-H}](8)+\phi[\text{O}\delta\text{-C}\varepsilon\text{-H}](6)$	1291	--	$\phi[\text{H-C}\alpha\text{-C}\beta](19)+\nu[\text{C}\alpha\text{-C}\beta](14)+\nu[\text{C}\beta\text{-C}](13)+\phi[\text{C}\alpha\text{-C}\beta\text{-H}](10)+\phi[\text{H-C}\alpha\text{-C}\gamma](8)+\phi[\text{H-C}\beta\text{-C}](5)$
1281	1278	$\phi[\text{H-C}\eta\text{-C}\xi](14)+\phi[\text{C}\varepsilon\text{-C}\eta\text{-H}](13)+\phi[\text{H-C}\alpha\text{-C}\beta](10)+\phi[\text{O}\delta\text{-C}\varepsilon\text{-H}](9)+\nu[\text{C}\alpha\text{-C}\beta](8)+\phi[\text{H-C}\varepsilon\text{-C}\eta](7)$	1282	1278	$\phi[\text{H-C}\eta\text{-C}\xi](26)+\phi[\text{C}\varepsilon\text{-C}\eta\text{-H}](24)+\phi[\text{O}\delta\text{-C}\varepsilon\text{-H}](16)+\phi[\text{H-C}\varepsilon\text{-C}\eta](13)+\phi[\text{H-C}\xi\text{-C}\chi](7)+\phi[\text{C}\eta\text{-C}\xi\text{-H}](6)$
1203	1198	$\phi[\text{C}\alpha\text{-C}\beta\text{-H}](22)+\phi[\text{H-C}\alpha\text{-C}\gamma](17)+\phi[\text{H-C}\beta\text{-C}](17)+\phi[\text{H-C}\alpha\text{-C}\beta](14)+\nu[\text{N-C}\alpha](11)+\nu[\text{C}\beta\text{-C}](8)$	1205	1198	$\phi[\text{C}\alpha\text{-C}\beta\text{-H}](19)+\phi[\text{H-C}\alpha\text{-C}\gamma](16)+\phi[\text{H-C}\beta\text{-C}](15)+\phi[\text{H-C}\alpha\text{-C}\beta](14)+\nu[\text{C}\beta\text{-C}](10)+\nu[\text{N-C}\alpha](10)$
835	830	$\nu[\text{C}\gamma\text{-O}\delta](16)+\nu[\text{C}\eta\text{-C}\xi](12)+\phi[\text{C}\alpha\text{-C}\beta\text{-H}](12)+\phi[\text{H-C}\beta\text{-C}](8)+\phi[\text{C}\xi\text{-C}\chi\text{-H}](8)+\nu[\text{C}\alpha\text{-C}\gamma](7)+\omega[\text{C}=\text{O}](6)+\nu[\text{O}\delta\text{-C}\varepsilon](5)$	834	830	$\nu[\text{C}\gamma\text{-O}\delta](17)+\nu[\text{C}\eta\text{-C}\xi](12)+\phi[\text{C}\alpha\text{-C}\beta\text{-H}](10)+\nu[\text{C}\alpha\text{-C}\gamma](9)+\phi[\text{C}\xi\text{-C}\chi\text{-H}](8)+\phi[\text{H-C}\beta\text{-C}](7)+\nu[\text{O}\delta\text{-C}\varepsilon](5)$
803	796	$\phi[\text{C}\alpha\text{-C}\beta\text{-H}](24)+\phi[\text{H-C}\beta\text{-C}](16)+\nu[\text{C}\alpha\text{-C}\gamma](14)+\nu[\text{C}\gamma\text{-O}\delta](11)+\omega[\text{C}=\text{O}](9)$	801	796	$\phi[\text{C}\alpha\text{-C}\beta\text{-H}](24)+\phi[\text{H-C}\beta\text{-C}](18)+\nu[\text{C}\gamma\text{-O}\delta](10)+\nu[\text{C}\alpha\text{-C}\gamma](10)+\omega[\text{C}=\text{O}](9)$
632	--	$\omega[\text{C}\gamma=\text{O}\gamma](30)+\omega[\text{N-H}](16)+\phi[\text{C}\gamma\text{-C}\alpha\text{-C}\beta](9)$	642	--	$\omega[\text{N-H}](30)+\omega[\text{C}\gamma=\text{O}\gamma](15)+\phi[\text{C}\gamma\text{-C}\alpha\text{-C}\beta](6)+\omega[\text{C}=\text{O}](6)$
593	601	$\omega[\text{N-H}](20)+\omega[\text{C}\gamma=\text{O}\gamma](16)+\phi[\text{O}=\text{C-N}](8)+\nu[\text{C}\beta\text{-C}](7)+\phi[\text{C}\alpha\text{-C}\beta\text{-C}](6)+\phi[\text{C}\beta\text{-C}=\text{O}](5)$	602	601	$\omega[\text{C}\gamma=\text{O}\gamma](21)+\omega[\text{N-H}](10)+\omega[\text{C}=\text{O}](8)+\phi[\text{O}=\text{C-N}](6)+\tau[\text{N-C}\alpha](5)$
525	513	$\phi[\text{O}\gamma=\text{C}\gamma\text{-O}\delta](26)+\omega[\text{C}=\text{O}](18)+\phi[\text{C}\gamma\text{-O}\delta\text{-C}\varepsilon](12)+\phi[\text{C}\alpha\text{-C}\gamma\text{-O}\delta](9)+\phi[\text{N-C}\alpha\text{-C}\gamma](6)$	521	513	$\omega[\text{C}=\text{O}](23)+\phi[\text{C}\alpha\text{-C}\gamma\text{-O}\delta](11)+\phi[\text{O}\gamma=\text{C}\gamma\text{-O}\delta](10)+\phi[\text{N-C}\alpha\text{-C}\gamma](9)+\phi[\text{O}=\text{C-N}](8)+\phi[\text{C}\gamma\text{-O}\delta\text{-C}\varepsilon](7)$
472	474	$\phi[\text{C}\alpha\text{-C}\gamma=\text{O}\gamma](22)+\phi[\text{N-C}\alpha\text{-C}\gamma](9)+\phi[\text{C}\alpha\text{-C}\gamma\text{-O}\delta](9)+\phi[\text{O}\delta\text{-C}\varepsilon\text{-C}\eta](8)+\phi[\text{C}\beta\text{-C-N}](8)+\phi[\text{N-C}\alpha\text{-C}\beta](6)+\phi[\text{C}\beta\text{-C}=\text{O}](5)$	467	474	$\phi[\text{C}\alpha\text{-C}\gamma=\text{O}\gamma](20)+\phi[\text{C}\beta\text{-C}=\text{O}](10)+\phi[\text{O}\delta\text{-C}\varepsilon\text{-C}\eta](7)+\phi[\text{O}\gamma=\text{C}\gamma\text{-O}\delta](7)+\phi[\text{N-C}\alpha\text{-C}\gamma](7)+\phi[\text{C}\alpha\text{-C}\gamma\text{-O}\delta](6)+\phi[\text{C}\beta\text{-C-N}](6)$
366	--	$\phi[\text{C}\eta\text{-C}\xi\text{-C}\chi](35)+\phi[\text{O}\delta\text{-C}\varepsilon\text{-C}\eta](20)+\phi[\text{N-C}\alpha\text{-C}\beta](5)$	373	--	$\phi[\text{C}\eta\text{-C}\xi\text{-C}\chi](19)+\phi[\text{O}\delta\text{-C}\varepsilon\text{-C}\eta](17)+\phi[\text{C}\beta\text{-C-N}](6)+\phi[\text{N-C}\alpha\text{-C}\beta](5)$
355	--	$\phi[\text{O}=\text{C-N}](10)+\phi[\text{C}\beta\text{-C-N}](9)+\phi[\text{C}\varepsilon\text{-C}\eta\text{-C}\xi](8)+\phi[\text{N-C}\alpha\text{-C}\beta](8)+\phi[\text{C}\gamma\text{-C}\alpha\text{-C}\beta](8)+\tau[\text{C}\gamma\text{-O}\delta](7)+\phi[\text{C}\alpha\text{-C}\gamma=\text{O}\gamma](6)+\phi[\text{C}\eta\text{-C}\xi\text{-C}\chi](5)$	358	--	$\phi[\text{C}\eta\text{-C}\xi\text{-C}\chi](18)+\phi[\text{C}\alpha\text{-C}\gamma=\text{O}\gamma](10)+\phi[\text{N-C}\alpha\text{-C}\beta](9)+\phi[\text{C}\varepsilon\text{-C}\eta\text{-C}\xi](8)+\phi[\text{O}=\text{C-N}](5)$
321	--	$\phi[\text{C}\varepsilon\text{-C}\eta\text{-C}\xi](21)+\phi[\text{N-C}\alpha\text{-C}\gamma](19)+\phi[\text{O}\delta\text{-C}\varepsilon\text{-C}\eta](12)$	322	--	$\phi[\text{C}\varepsilon\text{-C}\eta\text{-C}\xi](24)+\phi[\text{O}\delta\text{-C}\varepsilon\text{-C}\eta](15)+\phi[\text{N-C}\alpha\text{-C}\gamma](11)+\phi[\text{C}\gamma\text{-O}\delta\text{-C}\varepsilon](5)$
269	--	$\phi[\text{C}\beta\text{-C}=\text{O}](17)+\tau[\text{C}\beta\text{-C}](13)+\phi[\text{N-C}\alpha\text{-C}\beta](9)+\phi[\text{C}\beta\text{-C-N}](9)+\phi[\text{C}\gamma\text{-C}\alpha\text{-C}\beta](8)+\phi[\text{C}\alpha\text{-C}\beta\text{-C}](5)$	307	--	$\phi[\text{N-C}\alpha\text{-C}\beta](18)+\tau[\text{C}\beta\text{-C}](13)+\phi[\text{C}\beta\text{-C-N}](8)+\phi[\text{C}\beta\text{-C}=\text{O}](7)+\phi[\text{C}\alpha\text{-C}\gamma=\text{O}\gamma](5)$
242	--	$\tau[\text{C}\xi\text{-C}\chi](47)+\tau[\text{C}\gamma\text{-O}\delta](16)+\phi[\text{N-C}\alpha\text{-C}\beta](8)$	240	--	$\tau[\text{C}\xi\text{-C}\chi](50)+\tau[\text{C}\gamma\text{-O}\delta](13)+\tau[\text{C}\alpha\text{-C}\gamma](8)+\tau[\text{C}\varepsilon\text{-C}\eta](6)$
237	--	$\phi[\text{N-C}\alpha\text{-C}\beta](19)+\tau[\text{C}\alpha\text{-C}\gamma](16)+\tau[\text{C}\xi\text{-C}\chi](9)+\phi[\text{C-N-C}\alpha](8)+\phi[\text{O}=\text{C-N}](7)+\phi[\text{C}\alpha\text{-C}\beta\text{-C}](6)$	217	--	$\phi[\text{C}\alpha\text{-C}\gamma=\text{O}\gamma](14)+\phi[\text{C}\gamma\text{-O}\delta\text{-C}\varepsilon](9)+\phi[\text{C}\alpha\text{-C}\beta\text{-C}](8)+\phi[\text{N-C}\alpha\text{-C}\gamma](7)+\phi[\text{C}\eta\text{-C}\xi\text{-C}\chi](5)$
211	--	$\phi[\text{C}\alpha\text{-C}\gamma=\text{O}\gamma](19)+\phi[\text{C}\gamma\text{-O}\delta\text{-C}\varepsilon](11)+\nu(53)+\phi[\text{C}\beta\text{-C}=\text{O}](7)+\phi[\text{C}\beta\text{-C-N}](7)+\phi[\text{C-N-C}\alpha](5)+\phi[\text{C}\alpha\text{-C}\gamma\text{-O}\delta](5)$	184	--	$\tau[\text{C}\alpha\text{-C}\gamma](8)+\phi[\text{C-N-C}\alpha](8)+\phi[\text{C}\beta\text{-C}=\text{O}](8)+\phi[\text{C}\beta\text{-C-N}](8)+\phi[\text{C}\varepsilon\text{-C}\eta\text{-C}\xi](7)+\phi[\text{N-C}\alpha\text{-C}\beta](7)+\tau[\text{C}\beta\text{-C}](6)+\phi[\text{C}\gamma\text{-C}\alpha\text{-C}\delta](6)$
143	--	$\phi[\text{C}\gamma\text{-C}\alpha\text{-C}\beta](16)+\tau[\text{C}\alpha\text{-C}\gamma](7)+\tau[\text{C}\varepsilon\text{-C}\eta](6)+\phi[\text{C}\alpha\text{-C}\beta\text{-C}](6)+\tau[\text{C}\beta\text{-C}](6)+\tau[\text{C}\gamma\text{-O}\delta](5)$	145	--	$\phi[\text{C}\alpha\text{-C}\beta\text{-C}](11)+\phi[\text{C}\alpha\text{-C}\gamma\text{-O}\delta](8)+\phi[\text{C}\varepsilon\text{-C}\eta\text{-C}\xi](8)+\tau[\text{C}\alpha\text{-C}\gamma](7)+\phi[\text{C}\gamma\text{-C}\alpha\text{-C}\beta](7)$
102	--	$\tau[\text{C}\varepsilon\text{-C}\eta](21)+\tau[\text{C}\alpha\text{-C}\gamma](10)+\phi[\text{C}\alpha\text{-C}\beta\text{-C}](6)+\phi[\text{C}\gamma\text{-O}\delta\text{-C}\varepsilon](5)$	97	--	$\tau[\text{C}\varepsilon\text{-C}\eta](29)+\tau[\text{C}\gamma\text{-O}\delta](17)+\tau[\text{C}\alpha\text{-C}\gamma](7)$
85	--	$\tau[\text{C}\gamma\text{-O}\delta](17)+\phi[\text{C}\gamma\text{-O}\delta\text{-C}\varepsilon](10)+\tau[\text{C}\varepsilon\text{-C}\eta](10)+\phi[\text{O}\delta\text{-C}\varepsilon\text{-C}\eta](9)+\tau[\text{C}\alpha\text{-C}\beta](8)$	86	--	$\phi[\text{C}\gamma\text{-O}\delta\text{-C}\varepsilon](13)+\tau[\text{C}\beta\text{-C}](11)+\phi[\text{O}\delta\text{-C}\varepsilon\text{-C}\eta](9)+\tau[\text{N-C}\alpha](6)+\phi[\text{C}\varepsilon\text{-C}\eta\text{-C}\xi](6)$
80	--	$\tau[\text{N-C}\alpha](25)+\tau[\text{C}\beta\text{-C}](17)+\tau[\text{C}\alpha\text{-C}\beta](9)+\tau[\text{C}\gamma\text{-O}\delta](7)+\tau[\text{O}\delta\text{-C}\varepsilon](5)$	74	--	$\tau[\text{N-C}\alpha](18)+\tau[\text{C}\alpha\text{-C}\beta](18)+\tau[\text{C}\beta\text{-C}](8)$
66	--	$\phi[\text{C}\alpha\text{-C}\beta\text{-C}](10)+\phi[\text{C-N-C}\alpha](9)+\tau[\text{O}\delta\text{-C}\varepsilon](9)+\phi[\text{C}\gamma\text{-O}\delta\text{-C}\varepsilon](8)+\tau[\text{C}\alpha\text{-C}\gamma](7)+\tau[\text{C}\gamma\text{-O}\delta](6)+\phi[\text{O}\delta\text{-C}\varepsilon\text{-C}\eta](5)+\phi[\text{C}\gamma\text{-C}\alpha\text{-C}\beta](5)+\phi[\text{C}\beta\text{-C-N}](5)+\phi[\text{C}\alpha\text{-C}\gamma\text{-O}\delta](5)$	65	--	$\tau[\text{O}\delta\text{-C}\varepsilon](19)+\tau[\text{C}\alpha\text{-C}\gamma](10)+\phi[\text{C}\gamma\text{-C}\alpha\text{-C}\beta](9)+\tau[\text{C}\beta\text{-C}](9)+\tau[\text{C}\gamma\text{-O}\delta](8)+\tau[\text{C}\eta\text{-C}\xi](8)$
28	--	$\tau[\text{C}\alpha\text{-C}\gamma](18)+\tau[\text{O}\delta\text{-C}\varepsilon](12)+\omega[\text{C}\gamma=\text{O}\gamma](10)+\tau[\text{C}\gamma\text{-O}\delta](8)+\phi[\text{C}\gamma\text{-O}\delta\text{-C}\varepsilon](6)+\phi[\text{N-C}\alpha\text{-C}\gamma](6)$	30	--	$\phi[\text{C}\gamma\text{-O}\delta\text{-C}\varepsilon](14)+\phi[\text{C}\alpha\text{-C}\gamma\text{-O}\delta](12)+\phi[\text{N-C}\alpha\text{-C}\gamma](7)+\omega[\text{C}\gamma=\text{O}\gamma](6)+\phi[\text{C}\gamma\text{-C}\alpha\text{-C}\beta](6)$
15	--	$\phi[\text{C}\alpha\text{-C}\gamma\text{-O}\delta](12)+\phi[\text{C}\gamma\text{-O}\delta\text{-C}\varepsilon](8)+\phi[\text{C}\alpha\text{-C}\beta\text{-C}](7)+\omega[\text{C}\gamma=\text{O}\gamma](7)+\tau[\text{C}\alpha\text{-C}\beta](7)+\phi[\text{C}\gamma\text{-C}\alpha\text{-C}\beta](5)$	15	--	$\tau[\text{C}\alpha\text{-C}\gamma](12)+\omega[\text{C}\gamma=\text{O}\gamma](11)+\phi[\text{N-C}\alpha\text{-C}\gamma](7)+\tau[\text{C}\gamma\text{-O}\delta](7)+\omega[\text{N-H}](6)+\tau[\text{O}\delta\text{-C}\varepsilon](6)+\phi[\text{C}\gamma\text{-C}\alpha\text{-C}\beta](5)$

Note: All frequencies are in wavenumbers (cm^{-1}).

3.3. Other Skeletal Modes

In the backbone of PANBLA, one methylene unit is attached, which provides greater conformational versatility to the chain of the polymer. The asymmetric, symmetric stretch, and scissoring modes of the methylene group of backbone ($C_{\beta}H_2$) are calculated at 2899, 2859, and 1426 cm^{-1} respectively. The above modes lie in the same range in PAIBLA [11] and poly (4-methyl, 1-pentene) {P4MP1} [18]. These modes are highly localized and non-dispersive in nature. The modes calculated at 1283, 1208, 1057, 956 and 803 cm^{-1} at zone center are assigned to 1278, 1198, 1050, 960 and 796 cm^{-1} respectively. These are wagging (1283 cm^{-1}), twisting (1057 cm^{-1}), and rocking modes (956, 803 cm^{-1}) of this CH_2 group. The mode at 1208 cm^{-1} is mixed wag and twist. These lie in the same range as observed in other systems such as PAIBLA [11] and P4MP1 [18].

3.4. Side Chain Modes

PANBLA has a bulky side chain, which consists of an ester group with a terminating *n*-butyl group. The pure side chain modes are non-dispersive and are given in Table 3. The three CH_2 groups of side chain are anchored by $O=C-O$ group at one end and flexible CH_3 group at the other end.

The asymmetric and symmetric stretches of CH_3 group are calculated at 2963 and 2923 cm^{-1} and assigned to the observed peaks at 2967 and 2923 cm^{-1} respectively. The degenerate antisymmetric deformation mode of CH_3 group is calculated at 1458 and 1450 cm^{-1} and assigned to the observed peak at 1468 cm^{-1} . Similar modes are observed at 1465 cm^{-1} in PAIBLA [11]. The peak observed at 1392 cm^{-1} corresponds to the symmetric deformation mode observed 1396 cm^{-1} . The CH_3 rocking mode calculated at 1028 cm^{-1} is assigned to the observed peak at 1022 cm^{-1} .

The mode calculated at 1750 cm^{-1} (assigned at the same value) has dominant contribution of stretching of $C=O_{\gamma}$. The same mode appears at 1747 and 1751 cm^{-1} in PAIBLA (hexagonal and tetragonal respectively). So it is evident that this mode is localized in nature. The out of plane bending of $C_{\gamma}=O_{\gamma}$ group have been calculated at 632 and 601 cm^{-1} . The zone center mode at 1105 cm^{-1}

having main contribution of $\nu(C_{\gamma}=O_{\gamma})$ of carbonyl group is assigned to observed peak at 1108 cm^{-1} .

3.5. CH_2 Group Modes

The side chain of PANBLA having three CH_2 groups is flanked by rigid $O=C-O$ group at one end and flexible CH_3 group at the other end (treated free). The frequencies of the CH_2 groups in side chain are compared with those observed by applying the selection rules (Table 7). The normal modes for finite linear chain of CH_2 groups have selection rules different from those for infinite chain. They are related to the dispersion of corresponding normal modes in infinite chain (polyethylene (PE) in this case) [19, 20] and corresponding absorption/scattering occurs at phase values given by [21] for one end fixed and the other end free:

$$d = \frac{(2k-1) \cdot p}{2(m+1)} \quad (5)$$

where m is the number of CH_2 groups (three here) and $k=1, 2, 3, 4$.

These allowed values of d for a given mode would give rise to frequencies, which fall on the corresponding dispersion curves (PE in this case) for an infinite system. These allowed values of d and corresponding frequencies are shown in Figs. 6 and 7. The correlation between frequencies obtained from dispersion curves of PE and the corresponding modes observed in CH_2 groups of PANBLA for scissoring, wagging, twisting, rocking, and C-C stretching modes are summarized in Table 7. Except C-C stretch, other modes are in agreement with those calculated from the dispersion curves of PE. Small deviations could arise because of intra and interchain interactions of CH_2 groups with ester and other groups. The asymmetric and symmetric CH_2 stretch modes are calculated at around 2895 and 2865 cm^{-1} . Some modes of CH_2 groups show a larger spread and the closeness of some components of the observed wave numbers contributes to line width and asymmetry. From Table 7 it is evident that all modes except C-C stretch are close to the calculated values from PE dispersion curves. Normally the presence of COO group at one end would result in a charge distribution with higher frequency but the calculated lower frequency indicates a strong coupling along the side chain.

Table 5

Comparison of amide modes of PANBLA with other w-helices

Modes	PANBLA		PAIBLA		PBrBO		PLPA	
	$\delta = 0$	$\delta = 0.5\pi$						
Amide A	3287	3287	3310	3310	3320	3320	3317	3317
Amide I	1644	1643	1660	1660	1640	1640	1651	1651
Amide II	1548	1548	1550	1551	1528	1522	1542	1542
Amide III	1272	1265	1280	1286	1300	1300	1309	1309
Amide IV	668	662	579	594	613	640	700	684
Amide V	668	662	683	675	613	640	622	622
Amide VI	549	554	542	542	580	--	556	556

Notes: 1. All frequencies are in cm^{-1} . 2. PANBLA = poly(α -*n*-butyl- β -L-aspartate); PAIBLA = poly(α -isobutyl- β -L-aspartate) [11]; PBrBO = poly(N^{ϵ} -*p*-bromobenzyl-L-ornitine) [16]; PLPA = poly(L-phenylalanine) [17]

Table 6

Comparison of amide modes of PANBLA with PAIBLA (tetragonal and hexagonal Forms)

Modes	PANBLA	PAIBLA (tetragonal)	PAIBLA (hexagonal)
Amide A	3287	3310	3282
Amide I	1644	1660	1653
Amide II	1548	1551	1543
Amide III	1272	1280	1290
Amide V	668	683	676

Note: 1. All wavenumbers are in cm^{-1} . 2. * marked wavenumbers are observed in the spectra of polyethylene.

Table 7

Comparison of CH_2 modes (side chain) of PANBLA with those from dispersion curves of polyethylene (PE)

Modes	Calculated by selection rule from PE dispersion curves	PANBLA	
		Freq. (calc.)	Freq. (obs.)
CH_2 asymmetric stretch	2919*	2899	---
		2895	
		2889	
CH_2 symmetric stretch	2848*	2868	2864
		2867	
		2865	
CH_2 scissoring	1441 1443 1447	1475	1468
		1469	
		1456	
CH_2 wag	1341 1272 1205	1416	1393 1347 1278 1198
		1351	
		1281	
		1208	
CH_2 twist	1282 1254 1187	1281	1278 1248 1198
		1241	
		1208	
CH_2 rock	1018 913 781	1011	1020 876 830
		866	
		828	
C-C stretch	913 1043 1066	917	-- 960
		958	
		--	

Notes: 1. All frequencies are in cm^{-1} . 2. PANBLA= Poly (α -n-butyl- β -L-aspartate). 3. PAIBLA = Poly (α -isobutyl- β -L-aspartate).

3.6. Mixed Modes

The modes which have contributions from both backbone and side chain, are described as mixed modes. These are shown in Table 4. In most of the modes below 900 cm^{-1} there is strong coupling of backbone and side chain vibrations. The out-of-plane bending of $\text{C}\gamma=\text{O}\gamma$ group is calculated at 601 cm^{-1} (assigned to peak at 593 cm^{-1}). The COO in plane bending calculated at 525 cm^{-1} ($d=0$) is assigned to spectral peak at 513 cm^{-1} . As d increases, the contribution of angle bend of $\text{C}\gamma$ decreases. The energy of the above mode decreases up to $d=0.42p$ and after that it increases again. The mode calculated at 472 cm^{-1} match well with observed peak at 474 cm^{-1} . The energy of this mode continuously decreases with progressive value of d .

It is observed that mixed modes show more dispersion as compared to the main chain and side chain modes.

3.7. Characteristic Features of Dispersion Curves

The dispersive modes below 900 cm^{-1} are shown in Figs. 3a, 4a and 5a. These curves provide the information on the extent and degree of coupling between various normal modes. Characteristic feature of dispersion curves like repulsion and exchange of character between various pairs of modes are observed. Pairs of modes that repel are ($668, 632 \text{ cm}^{-1}$), ($280, 269 \text{ cm}^{-1}$), ($236, 225 \text{ cm}^{-1}$), ($210, 192 \text{ cm}^{-1}$) and ($85, 80 \text{ cm}^{-1}$). These occur in the

neighborhood of $d = 0.50p$, $d = 0.21p$, $d = 0.25p$, $d = 0.44p$, and $d = 0.35p$ respectively. Calculations show that these modes approach each other and PEDs of the two modes start mixing. At a particular value of d they exchange their character and then diverge. Such repulsions occur for modes belonging to same symmetry species. The regions of density-of-states where $d\omega/dK \rightarrow 0$ are akin to critical points are known as von Hove type singularities in lattice dynamics [22].

The modes at 668 and 632 cm^{-1} come close near the helix angle and then diverge. In the first mode the contribution of ω (N-H) and ω (C=O) decreases, while in the second one, the contribution of ω ($C\gamma=O\gamma$) decreases. The PED exchange takes place at $d = 0.50p$. At this value they exchange their PEDs and respective contributions increase up to the zone boundary. This interesting phenomenon of exchange of character may be viewed as the collision of the two phonons approaching each other and exchanging their energy and then moving apart.

In mode calculated at 525 cm^{-1} (at $d = 0$), the contribution of ω (C=O) increases and ϕ ($O\gamma=C\gamma-O\delta$) decreases with δ and curve attains a minimum at $d = 0.40p$. After this d value, the energy of this mode increases. This curve shows von-Hove type singularity.

The pair of modes at 366 and 355 cm^{-1} (at $d = 0$) shows parallelism and they disperse by nearly the same amount in the same phase. This parallelism indicates that the speed of the two optical phonons is the same.

In the pair of modes at 280 and 269 cm^{-1} , the mixing of PEDs starts at $d = 0.18p$ and exchange of character

takes place at $d = 0.25p$. The upper mode at 280 cm^{-1} is highly dispersive and it shows a dispersion of around 38 cm^{-1} at $d = p$.

The energy of mode at 236 cm^{-1} first decreases and comes closer to the lower mode at 225 cm^{-1} . The PEDs start mixing at $d = 0.17p$ and at $d = 0.20p$ they have common PEDs. After this d value they start repelling. Similarly the pair of modes at 210 and 192 cm^{-1} come closer and at $d = 0.43p$ mixing of PED starts. The zone center mode at 85 and 80 cm^{-1} move in parallel up to $d = 0.35p$ and after this they repel. The energy of upper mode increases while that of lower one decreases. The lower frequency modes are characteristics of the 4/1 helix chains. The two acoustic branches in the dispersion curves are similar in shape to the dispersion of these branches in other helical systems like PAIBLA [11-12].

3.8. Frequency Distribution Function and Heat Capacity

The state density distribution function, which expresses the way in which energy is distributed among various branches of normal modes, is obtained from the dispersion curves for isolated chain of PANBLA, and is shown in Figs. 3b, 4b and 5b. The peaks in the frequency distribution curves corresponding to the regions of high density-of-states compare well with the observed frequencies. The frequency distribution function can also be used to calculate the thermodynamical properties such as heat capacity, enthalpy changes, etc. We have calculated the heat capacity of PANBLA in the temperature range

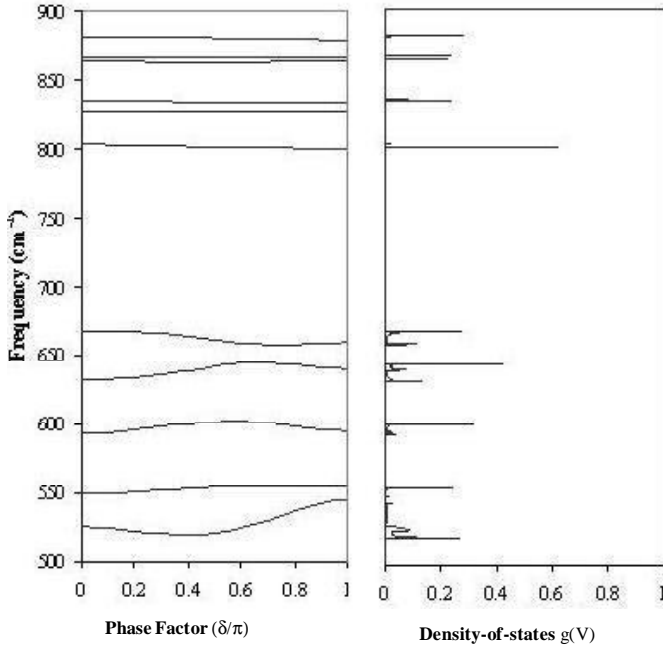


Fig. 3a. Dispersion Curves (500-900 cm^{-1})

Fig. 3b. Density-of-states (500-900 cm^{-1})

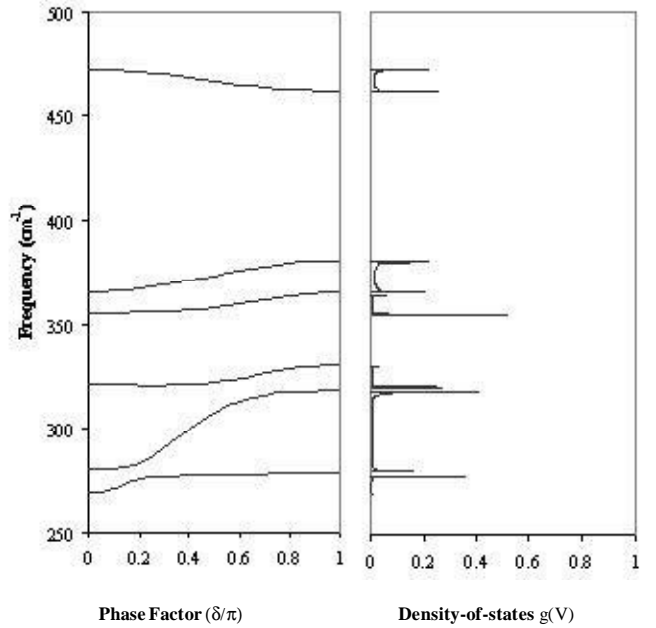


Fig. 4a. Dispersion Curves (500-250 cm^{-1})

Fig. 4b. Density-of-states (500-250 cm^{-1})

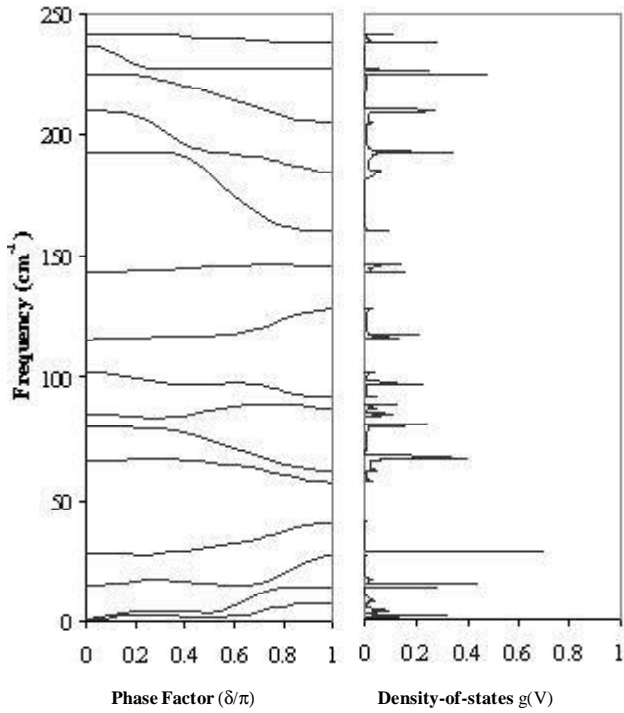


Fig. 5a. Dispersion Curves (below 250 cm⁻¹)

Fig. 5b. Density-of-states (below 250 cm⁻¹)

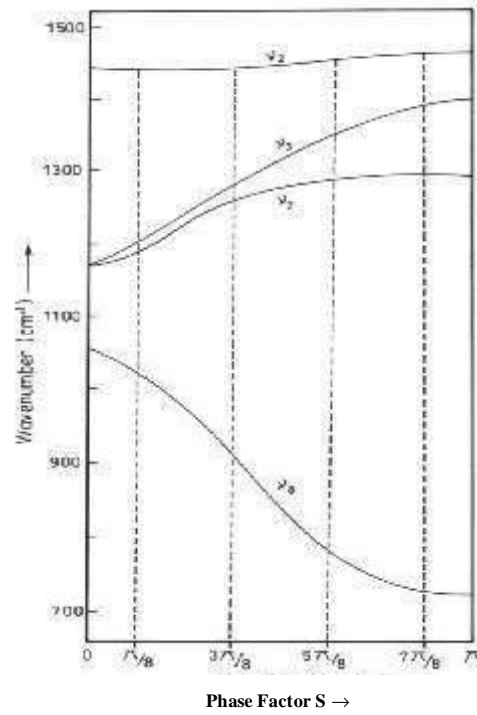


Fig. 6. Dispersion curve of the scissoring (v_2), wagging (v_3), twisting (v_7) and rocking (v_8) modes of polyethylene. — indicates the allowed phase values (δ)

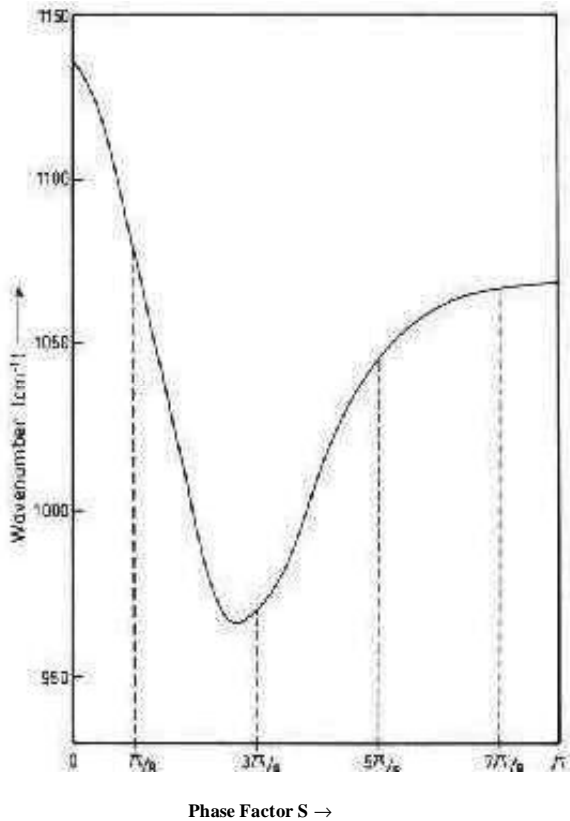


Fig. 7. Dispersion curves of the C-C stretching mode of polyethylene. — indicates the allowed phase values (δ)

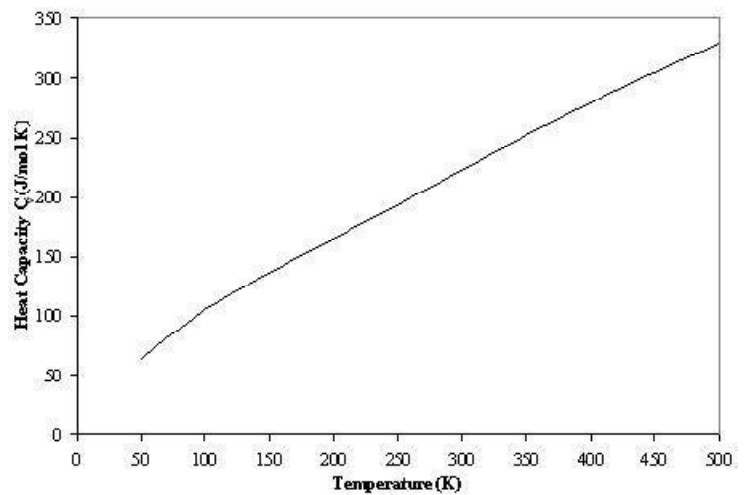


Fig. 8. Variation of heat capacity as a function of temperature

50–500 K. Since no experimental data is available at present, only predictive values are shown here (Fig 8). It is expected that these predictive values will stimulate experimental work on heat capacity.

In conclusion it may be mentioned that contribution from low frequency lattice modes is bound to make an appreciable difference in heat capacity due to sensitivity to these modes. In order to take into account this contribution, the dispersion curves have to be calculated for a three dimensional unit cell. In principle the evaluation of dispersion curves for 3D system is possible; however it would not make the problem intractable but also involve an enormous number of interactions, which are difficult to visualize and quantify. Due to these difficulties only normal mode contributions of a single chain to heat capacity are being calculated. In spite of several limitations involved and absence of experimental data, this work provides good starting point for more comprehensive studies of thermodynamical behaviour of polymeric systems under study.

Acknowledgements

One of the authors, Anuj Kumar would like to thank Dr. Y Meduri, COO Education, Jaypee Group & Dr. N. J. Rao, Director Jaypee Institute of Eng. & Technology, Guna for continuous encouragement and financial help throughout this work.

References

- [1] Bragg W., Kendrew J. and Perutz M.: Proc. Roy. Soc., A, 1950, **203**, 321.
- [2] Fernandez-Santin J., Guerra S., Rodriguez-Galan A. et al.: Macromolecules, 1987, **20**, 62.
- [3] Fernandez-Santin J., Aymami J., Rodriguez-Galan A. et al.: Nature, 1984, **311**, 53.
- [4] Lopez-Carrasquero F., Garcia-Alvarez M. and Guerra S.: Polymer, 1994, **35**, 4502.
- [5] Lopez-Carrasquero F., Martinez de Ilarduya A. and Guerra S.: Polymer, 1994, **26**, 694.
- [6] Lopez-Carrasquero F., Alvarez M., Ilarduya A. and Guerra S.: Macromol. Chem., Phys., 1995, **253**, 196.
- [7] Masamoto J., Sasaguri K., Ohizumi C. et al.: J. Appl. Polym. Sci., 1950, **14**, 667.
- [8] Guerra S., Fernandez-Santin J., Alegria C. and Subirana J.: Macromolecules, 1989, **22**, 5225.
- [9] Navas J., Aleman C., Lopez-Carrasquero F. and Munoz Guerra F.: Macromolecules, 1995, **28**, 13.
- [10] Carrasquero F., Aleman C. and Munoz Guerra S.: Biopolymers, 1995, **36**, 263.
- [11] Kumar A., Misra N., Kapoor D. et al.: Europ. Polym. J., 2001, **37**, 815.
- [12] Kapoor D., Kumar A., Misra N. et al.: Europ. Polym. J., 2001, **37**, 829.
- [13] Wilson E., Decius J. and Cross P.: Molecular vibrations: The theory of infrared & Raman Spectra. Dover Publications, New York 1980.
- [14] Higgs P.: Proc. Roy Soc., 1953, **220**, 472.
- [15] Mannfors B. and Krimm S.: J. Mol. Struct., 2000, **1**, 556.
- [16] Gupta A., Tandon P., Gupta V. D. and Gupta G. P.: J. Macromol. Sci. Phys. B, 1995, **34**, 500.
- [17] Burman L., Tandon P., Gupta V. D. and Srivastva S.: J. Macromol. Sci. Phys. B, 1995, **34**, 479.
- [18] Bahuguna G., Rastogi S., Tandon P. and Gupta V. D.: Polymer, 1996, **37**, 745.
- [19] Tasumi M. and Shimanouchi T.: J. Mol. Spectroscopy, 1962, **9**, 261.
- [20] Tasumi M. and Krimm S.: J. Chem. Phys., 1967, **46**, 755.
- [21] Zbinden R.: Infrared spectroscopy of high polymers. Academic Press, New York 1964.
- [22] Callaway J.: Quantum theory of solids. Academic Press, NY & London 1974.

ДИНАМІКА КОЛИВАНЬ

ПОЛІ(а-N-БУТИЛ-b-L-АСПАРТАТУ) (PANBLA)

Анотація. Вивчено полі(а-п-бутил-b-L-аспартат) (PANBLA), який є похідною Найлону-3, і в якому алкоксикарбонільна група стереорегулярно приєднана до b-вуглецю у ланці, що повторюється. Аналогічно полі(а-ізобутил-b-L-аспартату) (PAIBLA), досліджуваний полімер, який існує в двох спіральних формах, а саме в гексагональній (13/4 спіралі) і тетрагональній (4/1 спіралі), був охарактеризований рентген-дифракцією. Встановлено, що гексагональна форма, яка є мени кристалічною, не може бути отриманою достатньо орієнтованою, а тетрагональна – знаходиться у більш кристалічному стані. Молекулярні механічні розрахунки і середньо-квадратичний метод зв'язаних атомів з використанням рентген-дифракції свідчать про те, що антипаралельне укладання 13/4 спіралей з правосторонньою (2R) схемою водневих зв'язків більш придатне для гексагональної форми PANBLA. Тетрагональна форма сприяє паралельному розташуванню 4/1 спіралі відповідно до правосторонньої моделі 4R. Дослідження ІЧ-дихроїзму також підтверджують наведені результати. Хоча динаміка коливань обох форм PAIBLA була вивчена, для PANBLA такі дослідження не проводились.

В роботі приведені результати досліджень динаміки коливань для PANBLA в тетрагональній формі (4/1 спіралі) за допомогою дисперсії власних коливань. Крім детального опису власних коливань, пояснено характеристичні особливості дисперсійних кривих завдяки інтервальної симетрії в енергії імпульсного простору. Густина стану використовували для розрахунку теплоємності полімеру.

Ключові слова: полі(а-п-бутил-b-L-аспартат), густина стану, дисперсія фотонів, теплоємність.